The spin selectivity effect in chiral materials

D.H. Waldeck,[a] R. Naaman,[b] and Y. Paltiel[c]

a) Chemistry Department, University of Pittsburgh, Pittsburgh PA 15260 USA
b) Department of Chemical and Biological Physics, Weizmann Institute, Rehovot, 76100 Israel
c) Applied Physics Department and the Center for Nano-Science and Nano-Technology, The Hebrew University of Jerusalem, Jerusalem, 91904 Israel

Abstract

We overview experiments performed on the chiral induced spin selectivity (CISS) effect using various materials and experimental configurations. Through this survey of different material systems which manifest the CISS effect, we identify several attributes that are common to all the systems. Among these are the ability to observe spin selectivity for two point contacts configuration, when one of the electrode is magnetic, and the correlation between optical activity of the chiral systems and a material's spin filtering properties. In addition, recent experiments show that spin selectivity does not require pure coherent charge transport and the electron spin polarization persists over hundreds of nanometer in an ordered medium. Lastly, we point to several issues that still have to be explored regarding the CISS mechanism, among them the role of phonons and of electron-electron interactions.

I. Introduction

It is now well established that when electrons are transmitted through a chiral molecule, the transmission probability depends on the electron's spin state[1]. Namely, chiral molecules can serve as spin filters. This phenomenon, referred to as the chiral induced spin selectivity (CISS) effect,[2] has important implications across a range of scientific fields, including catalysis,[3] enantio-separation,[4] spintronics,[5] long range electron transfer,[6] bio-recognition,[7] and more. A growing number of research reports on CISS have probed its manifestation in chiral materials, including supramolecular assemblies, polymers, semiconductors, and semimetals. Understanding the structural and electronic origins of CISS in these materials, should provide a deeper understanding of the CISS mechanism and improve our ability to exploit the phenomenon in biological and technological applications.

Theoretical questions about the CISS effect remain substantial and it has been a challenge to model the phenomenon quantitatively.[8,9] An immediate and important question which needs to be answered through cooperation of theory and experiment is an understanding of structure-function relationships, i.e., how do features of the chiral system affect the efficiency of the spin polarization.[10] For example, experimental and theoretical studies both show that the spin polarization increases with molecular length, over the nm to tens of nm range, however no quantitative agreement between experiments and theoretical calculations exists. Other work presents a correlation of the spin selectivity observed in rate and transport measurements with a material's chiro-optical response,[11] these results are also not explained in most theories. Much theoretical work is still required to substantiate the existing observations and to guide experimental studies in ways that can distinguish among different theoretical descriptions.

An important, perhaps more fundamental question, is to what extent the CISS effect can be described by a single particle picture, or does it require electron-electron interactions and/or electron-phonon coupling. The experimentally observed correlation between a material's (or molecule's) optical activity and the spin filtering efficiency[11,12] suggests that the polarizability, and specifically the anisotropic polarizability, may play a role in chiral transport. Although not often discussed explicitly, most models assume that CISS proceeds coherently, however recent transport experiments report spin polarization for length scales of 100 nm to microns, which are too long for coherent transport to seem plausible.

Understanding the importance of coherence should help to elucidate the nature of CISS mechanism(s) and may prove useful in applying chiral materials to quantum sensing and quantum measurement applications. Simplified models, which apply orbital descriptions of the electronic structure and assume linear response, do not fully describe the experimental observations. While it is not yet clear what elements are needed for more sophisticated theoretical treatments, recent theoretical models that include electron-electron correlation[13,14] and/or electron phonon coupling[15,16] represent an important step forward in developing our understanding. First principles calculations promise to provide useful corroboration of experimental trends and insights into mechanism. Density functional theory (DFT) calculations comparing spin selectivity for helical (α-helix) versus nonhelical (β-strand) structures demonstrate the important impact of secondary structure on spin filtering efficiency,[17] and DFT results may provide a way to reveal the relative importance of the molecules intrinsic chirality and spin-orbit coupling from that imparted through coupling with the substrate/electrode material.[18] Such an achievement is likely to require a close cooperation between theory and experiment. The current range of experimental works, and the common features they display, can help guide the choice of model materials and systems for experimental and theoretical cooperation.

By reviewing the spin selectivity effect in a broad range of chiral materials, we aim to define what is known currently about the connection between material parameters and properties and how they affect spin selectivity. In the discussion, we sketch a mechanism of the CISS effect that we infer from the diversity of experiments.

II. Results

Probing the CISS effect requires that one's measurable quantity be sensitive to the electron's spin. These experiments can either probe directly the spin dependent current or can use another measurable quantity which depends on the spin polarization. Most measurements, which directly monitor the spin-dependent current, have used either a ferromagnetic electrode or some form of the Hall effect.[19,20] Often these measurements have been performed for molecules and materials at interfaces in order to control and limit orientational averaging of the spin-selectivity. These experiments can in principle probe single molecule or monolayers properties, when performed using STM and AFM for example, or they can probe bulk properties when studying crystals or thick films.

While spin polarized current measurements can depend sensitively on defining the measurement geometry in the laboratory frame, indirect measurements can be more lenient. For example, the impact of spin polarization on (electro-)catalysis for spin-dependent reactions will be sensitive to the local geometry of the reactants at the active site and their orientation relative to the chiral symmetry axis, but these need not be oriented in a particular direction in the lab frame. In what follows we will describe the experimental results for different classes of chiral molecules and materials in which the CISS effect was measured. The common effects to all systems will be highlighted in the last part of the manuscript.

Small Molecules, Monolayers and Oligomers

Numerous experiments have examined spin filtering in chiral molecules and their assemblies, including DNA, amino acids, oligopeptides, and helicenes. The discussion below divides these studies into those performed using photoelectron spectroscopy to measure the spin polarization of unbound electrons transmitted through monolayers adsorbed on a metal substrate, and those performed for electrons with energy below the vacuum level transmitted through molecules.

Unbound Photoelectrons

The CISS effect was observed first by the spin-dependent transmission yield of photoelectrons through monolayers of chiral fatty acids, stearoyl-lysine.[21] In these experiments, spin dependent injection of low energy electrons was realized by using circularly-polarized light to generate a spin-polarized photoelectron distribution from the substrate. The total spin dependent transmission was studied, but the spin of the electrons was not determined after they passed through the monolayer. A major development was the measurement of the spin of the transmitted electrons by use of Mott polarimetry.[22] In these studies, the spin of the electrons was determined after they passed through the chiral layer and it was found that their spin polarization was controlled by the molecular film's chirality.

It is important to appreciate that because the electrons' energy is low and the electrons are transmitted in the general direction perpendicular to the substrate, the electrons' wavelength perpendicular to their velocity, which is parallel to the substrate, is long. Hence, the transmitted electrons interact with more than one molecule in the

monolayer. This effect was indeed observed when monolayers were "doped" with molecules with the opposite handedness, and a relatively small fraction of doping caused the spin selectivity to drop considerably.[21]

The photoelectron studies have provided an important insight into the CISS mechanism. It was established that for a given family of oligomers, like peptides or DNA, the spin polarization depends nearly linearly on the length of the oligomer, for the first few nanometers.[22,23] In addition, it was found that the observed spin polarization for photoelectrons is affected only weakly by the substrate on which the molecules are adsorbed[24] and that the spin filtering of the photoelectrons becomes negligible at very high kinetic energy.[25] The photoelectron studies show that the chiral layer acts as a spin filter and the spin state of the electrons does not change while passing through the molecules, at least for the molecular lengths studied (< few nm).[26]

Bound electrons

Single molecules and monolayers studies: Studies include polypeptides, metal organics, amino acids, PNA, and DNA. Single molecule studies have been performed on peptides by applying the break junction concept, using STM.[27] Interestingly, although the electrons being conducted are bound, the results observed in terms of spin polarization are qualitatively similar to that observed with the photoelectrons. In these studies, the spin polarization is determined by making one of the electrode contacts magnetic. Surprisingly, although the Ni contact itself is known to have a spin polarization of only about 20% at room temperature, the spin polarization measured with the molecule(s) is much higher. Similar results have been reported in other studies,[28] and they suggest that the chiral molecule and the ferromagnetic spin filter cannot be considered as two independent linear filters. Rather, it suggests that the molecule/ferromagnet interfacial coupling is spin dependent; i.e., a 'spinterface'[29] forms. This hypothesis is substantiated by the experimental observation of spin polarized conduction (polarization ~ 100%) through a nickel oxide molecule located between two nickel contacts,[30] and the observation that the electron tunneling decay length into chiral molecule adlayers is spin dependent.[31] From this perspective, the large values of spin polarization observed in many CISS studies may well arise from the properties of the interface between the ferromagnet's surface layer and the molecule.

Another method of studying spin dependent conduction through one or a few molecules is the magnetic conducting probe-atomic force microscopy (mcAFM) method.[6] In this case the tip of an AFM is used to measure conduction through a molecule or several molecules adsorbed on a metallic substrate, in which either the AFM tip or the substrate is magnetized.[32] In either configuration, the spin-filtering has a similar dependence on magnetic field direction, current direction, and molecular chirality. As in the case of STM studies, the spin polarization values are similar to those obtained in photoelectron studies for the same molecules.[33]

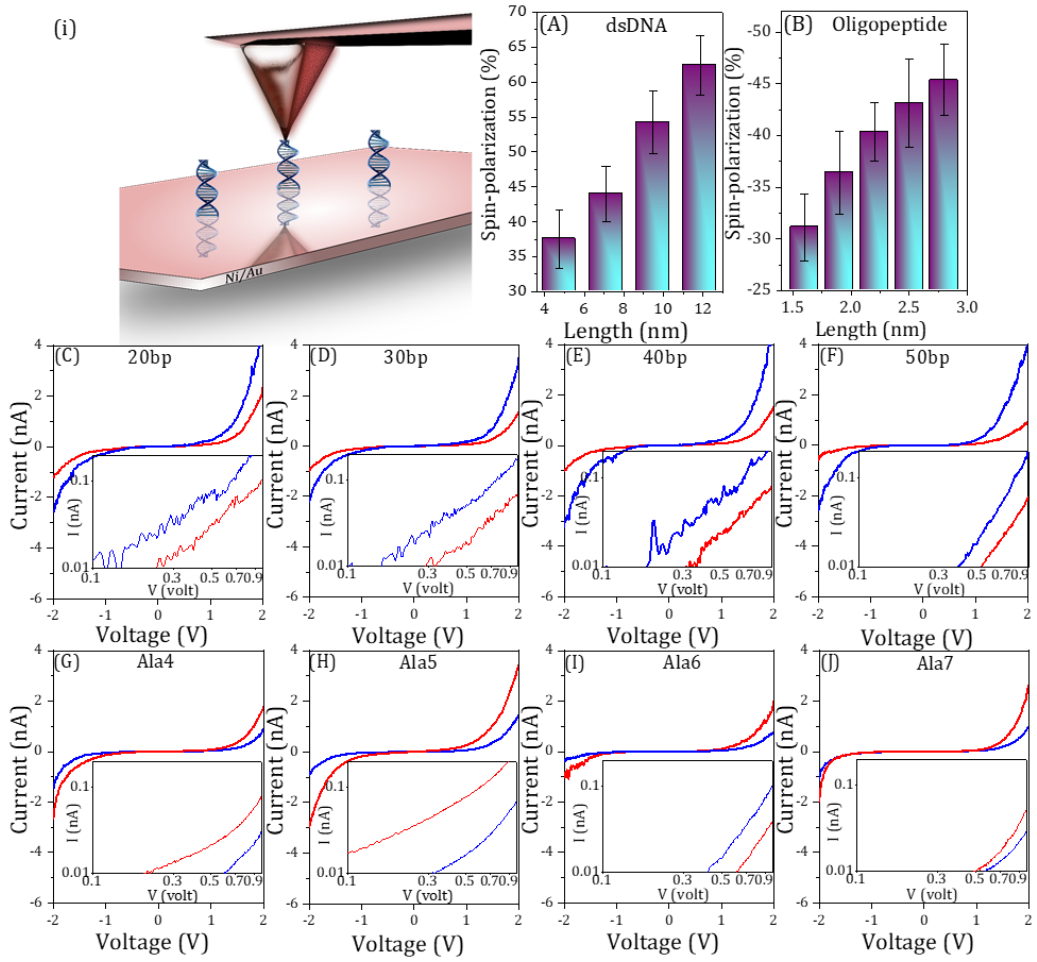

Figure 1: Results from the mcAFM measurements. (i) Schematic of the magnetic–conductive atomic force microscopy (mcAFM) set-up. (A, B) Histogram summary of spin polarization, P= $\{[(I_U - I_D)/(I_U + I_D)] \times 100\}$ for various lengths of dsDNA (A) and oligopeptide (B); the current I is measured at 2V. Panels C-F show the average current versus voltage curves obtained for oligomers of dsDNA with different numbers of base pairs (bp). Panels G-J present current-voltage curves for oligopeptides of different lengths. The inset in C through J shows the corresponding curves as a log-log plot. The blue curves correspond to the magnet North pole pointing UP, and the red curves correspond to the magnet North pole pointing DOWN. Copied with permission from ref. 33.

Fig. 1 shows magnetic conducting probe AFM measurements for duplex DNA oligomers (panels C to F) and for oligopeptides (panels G to J). These data reveal that the spin polarization increases monotonically with molecular length over this range of lengths. Moreover, the oligopeptides appear to be better spin filters per unit length than is the DNA; and the DNA and oligopeptides have opposite signs for their spin polarizations.

It is important to note that in all the studies described here, one electrode is magnetic and the other is not. The current versus voltage is measured typically when the magnetic electrode is magnetized with its spins aligned towards the chiral axis of the molecule versus away from it. In all these measurements, the magnetization direction that provides the higher current is the same for electrons moving away from the magnetic electrode and for electrons moving toward the magnetic electrode. Namely the preferred magnetization is the same for outgoing and ingoing current.

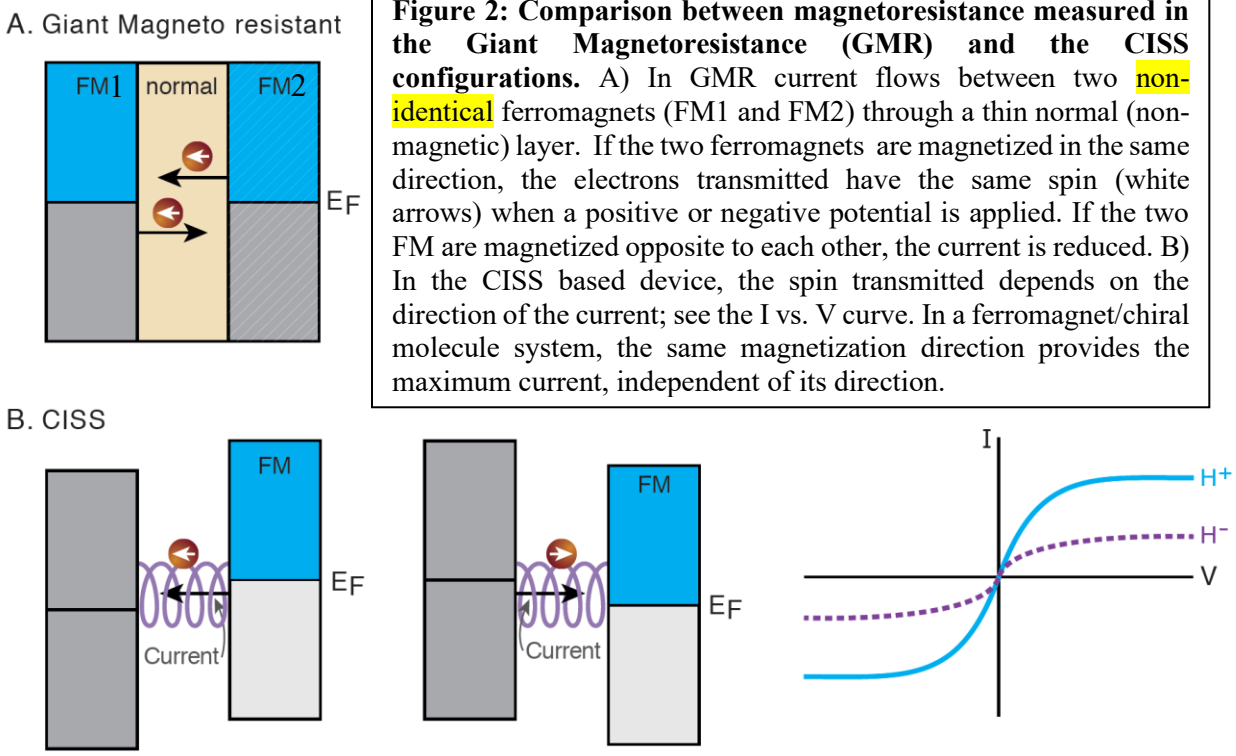

Figure 2: Comparison between magnetoresistance measured in the Giant Magnetoresistance (GMR) and the CISS configurations. A) In GMR current flows between two non-identical ferromagnets (FM1 and FM2) through a thin normal (non-magnetic) layer. If the two ferromagnets are magnetized in the same direction, the electrons transmitted have the same spin (white arrows) when a positive or negative potential is applied. If the two FM are magnetized opposite to each other, the current is reduced. B) In the CISS based device, the spin transmitted depends on the direction of the current; see the I vs. V curve. In a ferromagnet/chiral molecule system, the same magnetization direction provides the maximum current, independent of its direction.

The fact that the same magnet orientation relates to the maximum current, independent of the current direction, can be rationalized by consideration of the spin direction. In a typical achiral magnetoresistance device structure, the spin polarization is the same for current going both ways and it corresponds to the majority spin in the

ferromagnets. For example, Figure 2A shows a GMR thin film concept in which the two non-identical ferromagnetic (FM) layers are coupled through the thin nonmagnetic intermediary layer. Upon application of a magnetic field the FM magnetizations align and the spin filtering in such a device does not depend on the current direction.

For the case of current flow in a nonmagnetic electrode/chiral molecule/magnetic electrode structure (see Fig 2B. white arrows), the spin polarization flips upon changing the direction of the current. Namely, the electron current comprises the majority spins when flowing away from the ferromagnet (left part of 2B) and it comprises the minority spins when the electron current is flowing towards the ferromagnet (right part of 2B). This behavior results from the effective magnetic field the electron experiences, when flowing through a chiral potential. Hence, the symmetry associated with electron flow through a chiral system behaves like the magnetic field created due to current flowing through a coil. This magnetic field direction flips upon flipping the current direction and since the spin's magnetic dipole is affected by this effective magnetic field, the spin that is stabilized depends on the direction of the flow. Note that the time reversal symmetry is maintained because the current direction and the spin direction both flip sign whereas the magnetization of the electrode maintains its direction. This behavior is a signature of the CISS effect and should be captured by accurate theoretical treatments.

In most of the above systems the spin selectivity was measured using a two contact setup and large voltages. Although some simplified theoretical treatments predict that no spin filtering should occur in this configuration for the linear regime, namely when the current depends linearly on the applied voltage (low voltages),[34] experimental studies with chiral molecules display spin selectivity for two contact configurations at low voltages.[35] More recent theoretical descriptions, which account for one of the electrode's being magnetic and breaking time reversal symmetry, have pointed out that this configuration allows spin selectivity to manifest in a two electrode setup.[36,37]

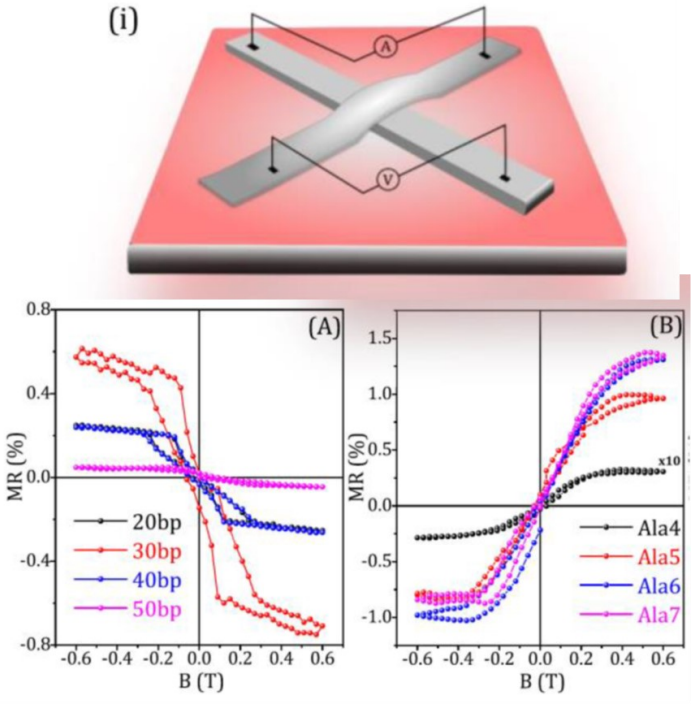

Figure 3: Magnetoresistance studies. (i) Schematic presentation of the magnetoresistance (MR) setup It is based on a 4-probe device fabricated on SiO_2. (A) MR results for various lengths of dsDNA, and (B) MR results obtained with different lengths of oligopeptides; results in both A and B were measured at 100 K. Copied with permission from Ref. 33.

A large number of studies, like that shown in Figure 1B, have been performed on monolayers or thin films located between two electrodes, one of them magnetic, in a two-point contact method.[38] These studies have also been performed using a four point contact configuration (see Figure 3), and the resistance of the chiral molecule layer is measured as a function of the magnetic field magnitude and direction (i.e., magnetoresistance).[39] The magnetoresistance in this case is antisymmetric with the field direction, in contrast to what is observed in GMR structures (Figure 2A). The antisymmetry versus the magnetic field, in the results of Fig. 3, arises because the spin current is affected by the chiral induced spin selectivity, arising from the chiral molecules, in addition to the effect of the magnetic field on the Ni film electrode. By way of example, consider the bottom right panel which shows a magnetoresistance curve for the oligopeptides. Under a negative magnetic field the magnetoresistance response is negative, indicating that R(H) is less than R(0), but under a positive field it is positive, indicating that R(H) is greater than R(0).

In addition to current-voltage measurements and magnetoresistance measurements for monolayer films of chiral molecules, other measurement methods have been used to probe the CISS response in molecules. The spin polarization that accompanies charge polarization has been studied using Hall devices.[40] Other studies have shown that the

adsorption of chiral molecules on a ferromagnetic film electrode induces a magnetization of the film.[41] The results indicate a strong coupling between the spin polarization in the molecules and the molecule's long axis, the coupling strength is significantly larger than k_BT at room temperature. The results support former studies which indicate that spin polarization in chiral molecules is accompanied by charge polarization and that the spins are strongly coupled to the molecular frame.[42,43] Spin transport through monolayers has been studied also using electrochemical cells, with the working electrode being magnetic.[44] This setup was used for examining spin dependent electron transfer rates through oligopeptides adsorbed on electrodes.[23,45] Collectively, these studies imply that the electron spin direction is coupled to the molecular frame in chiral molecules more strongly than the 'conventional wisdom' would imply.

Supramolecular structures and polymers: The synthesis, structural characterization, enantiospecific binding, and enantioselective chemistry of chiral supramolecular structures and polymers has been the focus of large research efforts.[46,47] The chirality in these systems can arise from point chirality of the monomers themselves and/or from axial chirality of the secondary structure. Indeed, the CISS effect was observed for both of these types of chiral polymers by using spin-specific electrochemistry methods, magnetic conducting probe measurements, and solid-state magnetoresistive device structures. In the first, the chiral polymer, poly{[methyl *N* -(tert-butoxycarbonyl)-S-3-thienyl- L -cysteinate]-cothiophene} was spread as thin films on a ferromagnetic substrate. In this case it was found that as long as the film thickness is small enough (typically below about 3 nm) spin polarization can be observed.[48] For thicker films, however, the spin polarization was degraded and it was attributed to scattering within the films. Interestingly, when polymers of poly(4-ethynylbenzoyl-L/D-alanine decyl ester) were adsorbed on the surface as a self-assembled monolayer, with the molecules long axis oriented perpendicular to the surface, spin polarization was observed even for monolayers of thickness ~6 nm.[49] These results underscore the importance of the order and/or the orientation of polymer molecules, through which the electrons are transmitted, in promoting spin polarization. In both cases, these polymers are made from monomers that are chiral and the polymerization generates a chiral secondary structure. The handedness of the secondary structure depends on the handedness of the monomers.

The study of supramolecular structures opens the possibility to investigate various architectures and to relate the spin polarization to the structural properties.[50] In most of these studies, the supramolecular structures formed long chains that were adsorbed with their chain axis along the magnetic substrate's surface, and the spin selective current was measured across the diameter of these wires. Two very interesting results emerged from these studies. The first is the observation of very high spin polarizations, exceeding 90% in some cases.[51] The second effect relates to the ability to combine chiral and achiral molecules in a supramolecular assembly that forms a chiral wire through the "sergeants and soldiers" effect, in which a small fraction of chiral molecules (the sergeants) induce the chiral arrangement of the achiral molecules (the soldiers) in the structure. This second aspect can be used to distinguish between the spin selectivity arising from the primary structure (point chirality) of the individual molecular components and that arising from the secondary structure (axial chirality) of the supramolecular assembly.

Kulkami et al[51] used the 'soldiers and sergeants' effect to examine the spin polarization in supramolecular chiral wires and its correlation with the chiro-optical response of the assemblies. They showed that the intensity of the circular dichroism (CD) spectra of the supramolecular wires increases in a nonlinear way with the addition of more and more sergeants, and that the spin polarization of electrons transmitted through these wires mimicked this behavior. The spin-filtering correlated with the oscillator strength of the lowest energy peak in the CD spectrum. Interestingly, this relation between the intensity of the CD spectra and the magnitude of the spin polarization has also been observed in the length dependent spin polarization studies performed on DNA and oligopeptides[33] and for the electron transfer rates in chiral quantum dots.[11,12]

The conclusions that have emerged from studying the polymers and the supramolecular structures is that the extent of spin polarization, arising from the CISS effect, is a non-local property. Namely, it results from the electronic properties of the system as a whole; for example, while the individual achiral monomers (the 'soldiers') do not necessarily manifest CISS individually, the coupling of their electronic response with the supramolecular chiral architecture and the subset of chiral monomers (the 'sergeants') combine to determine the overall spin polarization response.

Most of the experiments described above were performed when the electron is transported over lengths of a few nanometers or less. This length scale is comparable to the electron transfer ranges that have been studied for decades with molecules, and a complete theory of electron transfer and conduction through molecules should account for these chirality effects. Current electron transfer models do not include spin and chirality effects, however recent experiments imply that CISS can be important for spin chemistry[52] and enantioselectivity[53] and the model should be extended. The failure of the single electron theories and *ab initio* descriptions to quantitatively account for the magnitude of CISS effects is motivating researchers to pursue descriptions that move beyond the single electron models; and at some point these developments will need to be connected to existing electron transfer models, which are so successful for achiral systems. Further motivation for the development of more elaborate theoretical descriptions arises from spin transport measurements through chiral films and crystals with thicknesses of a few hundreds of nanometers, *vide infra*.

Metal-organic crystals and hybrid organic-inorganic perovskite films

Hybrid organic-inorganic materials represent a promising new direction for CISS studies. In experiments performed with two dimensional chiral crystals of perovskites[19,54,55] spin polarization approaching 100% was observed at room temperature. So far, we know about a single CISS related experiment that was performed on MOF crystals.[28] The crystal sizes were in some cases as big as 1 μm. In this case, spin polarization reaching 100% was reported. In another study, spin transport through chiral metal-organic crystals of copper phenylalanine were investigated and compared with crystals made from the perfluorinated phenylalanine molecules.[56] Interestingly, the preferred spin is opposite for L-phenylalanine and L-perfluorinated phenyl alanine. In both cases, the spin-selectivity correlates with the CD spectral response, because the sign of the CD response also flips upon fluorination.

Figure 4 presents the spin dependent conduction through copper phenylalanine crystals, measured with magnetic conducting AFM (mcAFM). The spin selectivity was observed for crystals of hundreds of nanometers at room temperature. Based on the CISS effect alone, the current magnitude for the L-enantiomer with the up-magnetized substrate should

be the same as that for the D-enantiomer with the down-magnetized substrate. Figure 4 shows that this is not the case. Instead, for Phe-Cu (F_5Phe-Cu) the current measured with the L enantiomer is generally higher (lower) than for the D enantiomer. This can be rationalized by the observed room-temperature ferromagnetism of the phenylalanine

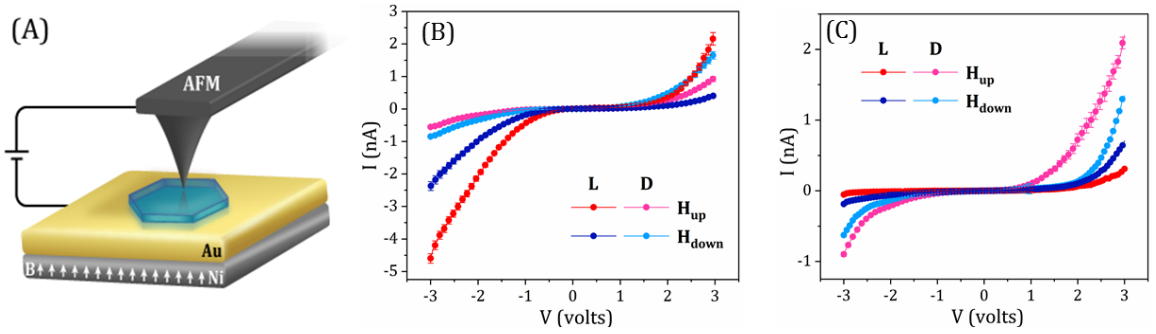

Figure 4. Spin-selective conduction through metallo-organic crystals. **(A)** Schematic of the mc-AFM measurement setup. A ~300 nm thick sample (blue hexagon) is placed on a gold-coated Ni surface and contacted from above by a conducting AFM tip. The substrate is magnetized with an external magnetic field of about 200 Oe. **(B, C)** Room-temperature current-voltage (I-V) measurements of D- and L-Phe-Cu (**B**) and D- and L-F_5Phe-Cu crystals (**C**), showing spin-selective conduction that depends on enantiomer type, external field direction, and bias polarity. The symbol size represents the measurement error. The measurements were performed at room temperature. Note that spin injected from the substrate is polarized in the opposite direction to the magnetic dipole of the substrate. (Copied with permission from ref. 56).

crystals. While the preferred spin injection depends on the handedness (L or D), the preferred spin transport also depends on the magnetization direction of the molecular ferromagnet, independent of chirality. Therefore, large current is observed only if both effects support the same spin preference. Hence, the combination of ferromagnetism and chirality provides an interesting variation on the typical CISS response.

Lu et al.[54] have used magnetic conducting probe and magnetoresistance measurements to demonstrate chiral induced spin selectivity in chiral hybrid organic-inorganic perovskites (HOIPS). In this work they applied an assembly method first developed by Ahn et al.[57] to fabricate thin (circa 50 nm) perovskite films and studied the spin dependent charge transport through them. Figure 5 shows magnetic conducting probe AFM data for chiral HOIP films. For example, panel B shows measurements for films with an R-chiral ligand incorporated between the perovskite sheets and displays a much higher conductance for a tip magnetized up than for a tip magnetized down. Panel D displays the opposite (mirror-image) behavior and corresponds to the case of an S-chiral ligand between

the perovskite sheets, whereas panel C represents a control experiment in which no chiral ligands are incorporated between the perovskite sheets. The spin polarization of the current, defined as $100\%\cdot(I_{up}-I_{down})/(I_{up}+I_{down})$, was found to be +86% for an R-HOIP film and −84% for an S-HOIP film at -2 V bias and that it displayed a weak dependence on the film thickness.

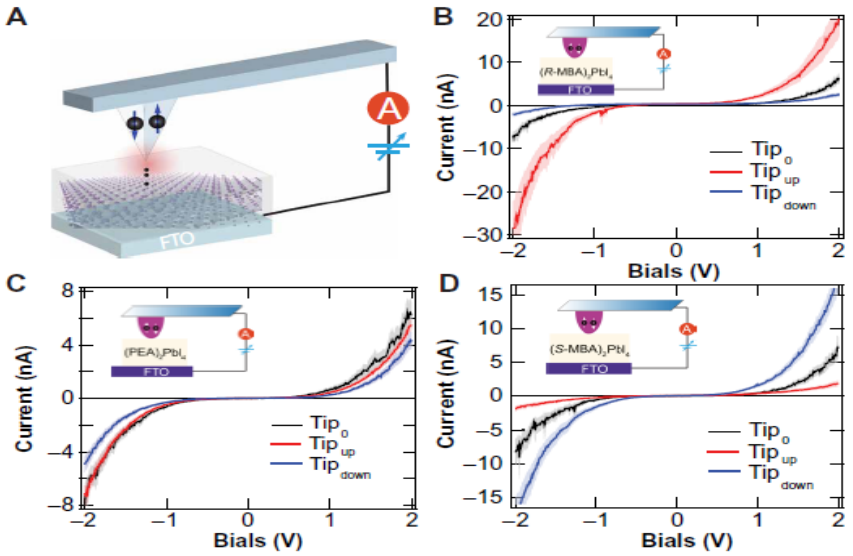

Figure 5: Schematic illustration of magnetic conductive AFM (mcAFM) measurements (A) and chirality dependence in out-of-plane charge transport (B to D) for perovskite films. Room-temperature I-V curves obtained using the mcAFM technique of chiral 2D hybrid perovskite thin films (~50 nm thick) for $(R\text{-MBA})_2PbI_4$ (B), $(S\text{-MBA})_2PbI_4$ (D), and nonchiral perovskite film PEA_2PbI_4 (C). The I-V curves are shown for the tip magnetized north (blue), magnetized south (red), and nonmagnetized (black). The I-V response for each 2D film was averaged over 100 scans, and the shaded region around the lines marks the 95% confidence limits for the average results. Copied with permission from Ref. 54 Figure 3.

Other experiments have revealed the manifestation of spin polarization and magneto-electrical responses in chiral perovskite films. For example, Lu et al[54] measured magnetoresistance data for HOIP films of the sort in Figure 5 and observed magnetoresistance versus magnetic field curves that display the same sort of antisymmetry as shown in Figure 3 for DNA and peptide oligomers. Interestingly, the authors measured the magnetoresistance as a function of the thickness of the chiral perovskite film and found that it increases, albeit modestly, with increasing thickness over the range of 20 nm to 100

nm. In a similar system, Huang et al[19] examined the magneto-optical Kerr effect in chiral HOIP/NiFe heterostructures. They showed that optical illumination of the chiral-HOIPs generates a magnetization on the underlying ferromagnetic substrate, and that the sign of the magnetization depends on the chirality of the HOIPs. It is important to note that this all-optical measurement method does not suffer from artifacts that might arise in electrical transport measurements, yet it corroborates the phenomena observed in those measurements. A number of studies (e.g., see 58,59,60) show the importance of spin-orbit coupling in achiral HOIPs and its impact on spin transport. In addition to providing a useful testbed for examining the relationship between chiral symmetry and spin-orbit coupling in materials, HOIP materials may also provide important demonstrations of the CISS effect in optoelectronic applications, such as spin light-emitting diodes.[61]

Inorganic crystals and oxides

The CISS effect has now been shown for three types of inorganic materials: chiral inorganic crystals, chiral nanoparticles, and chiral oxides. While chiral inorganic crystals, like quartz for example, are well known and have many technological applications, the use of chiral crystals as electron spin filters is new. Chiral oxides have a long history also and they manifest in bio-mineralization,[62,63] however their use in electronic applications has largely ignored their chirogenic properties. In the past two decades new synthetic methods have enabled research groups to investigate the CISS effect in chiral metal oxides.[64,65] Chiral inorganic nanoparticles are a relatively new type of material (first reported in 2007).[66,67,68] The ability to manipulate the chirality with organic surface ligands and control

optical and electronic properties through chemical composition and nanoparticle size make them excellent candidates for fundamental studies into CISS. Several models have been presented to explain this induced chirality and the subject is still under extensive research.

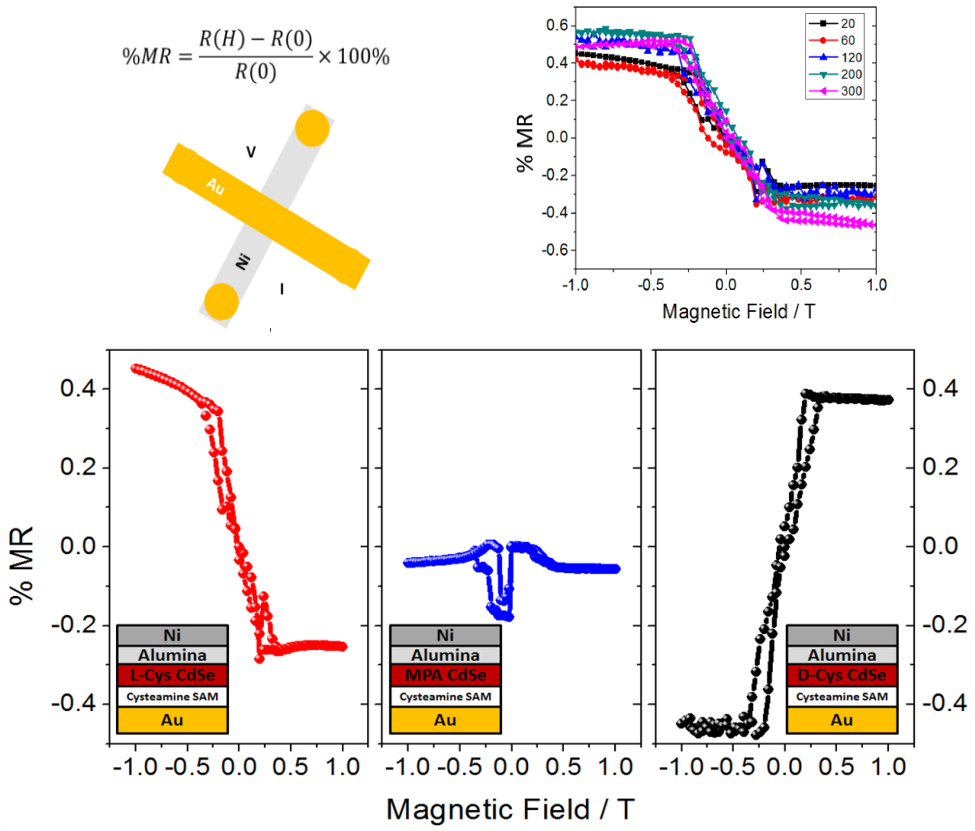

Figure 6: Magnetoresistance data for submonolayer films of CdSe quantum dots. The top left image illustrates the four-point probe measurement. The bottom panel shows the magnetoresistance response for the L-CdSe QD film on the left, an achiral CdSe QD film in the middle, and a D-CdSe QD film on the right. The top right curve shows the magnetoresistance response for the L-CdSe QD film at five different temperatures. Adapted with permission from reference 75.

In 2016 Bloom et al[69] used magnetic conducting probe measurements and magnetoresistance measurements to show that chiral quantum dots (QDs) can act as spin selective filters during charge transport. Figure 6 summarizes the magnetoresistance data for submonolayer films of chiral-imprinted CdSe QDs. The bottom panel shows magnetoresistance curves associated with three different magnetoresistor stacks, displayed in their insets. The panel in the bottom center uses achiral QDs, and it shows that a plot of

magnetoresistance versus magnetic field is symmetric in the field (i.e., the response depends on the magnitude of the field but does not change with the field direction - plus versus minus). The symmetry in %MR versus magnetic field curve arises because the response in this case arises from the splitting of the spin sublevels in the Ni film, whereas the other components of the magnetoresistor are not magnetic. In contrast to the achiral QD case, the chiral QDs display a response which is antisymmetric; i.e., it depends on the sign of the magnetic field. This antisymmetry arises because the spin current is affected by the chiral induced spin selectivity arising from the chiral QDs in addition to the effect of the magnetic field on the Ni film electrode, as described above in relation to Fig. 3.

The use of chiral QDs as electron spin filters promises new types of architectures for spin-based devices. Both the antisymmetric response for the magnetoresistance and the weak temperature dependence represent novel and useful attributes for applications. Bloom et al.[11,12] have shown that chiral QDs can be combined into supramolecular assemblies to introduce spin polarized photocurrent pathways, and they can be coupled with Hall device structures in interesting ways. For example, Al-Bustami et al[70] demonstrated an optical multilevel spin bit with a nine-state readout, that is based on chiral QDs and the chiral induced spin selectivity (CISS) effect.

Recently, Inui et al[71] have demonstrated spin-polarized currents in $CrNb_3S_6$ crystals, which are intrinsically chiral and highly conductive, under no external magnetic field. Their experimental design fabricated microscale electrical circuits with single crystals of $CrNb_3S_6$; see the top panel in Figure 7. Upon current injection into the chiral crystal, they were able to sense its spin polarization (via the CISS effect) through the use of a tungsten electrode which displays a strong inverse spin Hall response (a 'spin detection' electrode); see middle panel in Figure 7. The voltage versus current plot in the right middle panel shows how the Hall voltage signal changes with the applied current. The red, blue, and green plots correspond to different sizes and chirality for the crystals, and the crystal used to obtain the green data points has a chirality which is opposite to that used for the other two devices (red and blue data points). This represents the CISS phenomenon that has been observed in a number of other experiments. Because of the elegant device structure, they were also able to change the measurement protocol and inject a current into the tungsten electrode. This operation mode generates a voltage across the

electrodes on the two edges of the crystal, thus demonstrating an inverse CISS effect; i.e., by injecting a spin-polarized current through the device they were able to generate a voltage response.[72]

Recent work has also shown that chiral metal oxide films display spin filtering properties and these films have been used to affect the selectivity of chemical catalysis on the film surfaces. Ghosh et al. [73] prepared chiral CuO films by electrodeposition on a polycrystalline Au substrate and then used Mott polarimetry photoemission spectroscopy to show that the films spin polarize photoelectrons. They also used these CuO films as electrocatalysts for the oxygen evolution reaction. While it is well known that CuO is an effective electrocatalyst for the conversion of water to oxygen, that process also generates H_2O_2 as a side product. Because chiral CuO acts as a spin filter, it biases the electrochemical reaction toward the formation of the oxygen triplet product state over that

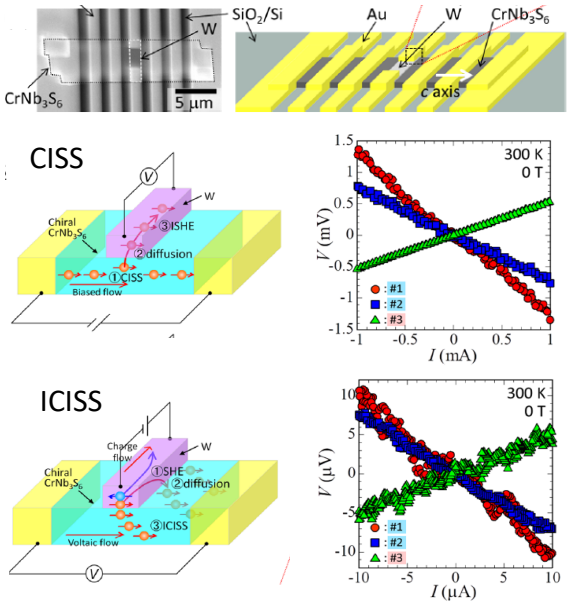

Figure 7. Top: The device is made of a $CrNb_3S_6$ strip with a tungsten electrode at the center and gold electrodes beside. An enlarged image on the upper right shows the area of the tungsten electrode edge, which is partially covered by the gold electrode. The c axis of $CrNb_3S_6$ is indicated by a white arrow. Current-voltage CISS and inverse CISS (ICISS) characteristics at 300 K at 0 Tesla are shown in the middle and bottom panels. For details see the text. Adapted with permission from Ref. 71.

for the formation of the hydrogen peroxide or singlet oxygen. While the measurements reveal a somewhat modest improvement in current efficiency, they display a nearly twenty-fold improvement in product selectivity. More recently, Ghosh et al[74] developed chiral cobalt oxide thin film electrocatalysts for the oxygen evolution reaction and examined how their spin polarization properties affect the reaction outcome. By creating a paramagnetic phase of the oxide and magnetizing it, they were able to independently show the impact of spin polarization on the photocurrent. These findings corroborate the effects found for the CuO electrocatalysts. For both the CuO and the CoOx chiral electrocatalyst films, the

improved performance was attributed to the formation of spin-polarized intermediates (OH radicals and O radicals) on the electrocatalyst surface during electrolysis, because of the chiral induced spin selectivity effect.

Similar high polarization was reported for chiral mesostructured NiO films.[75] In this case, chiral mesostructured NiO films were fabricated through the symmetry-breaking effect of a chiral molecule. Two levels of chirality were identified, primary nanoflakes with atomically twisted crystal lattices and secondary helical stacking of the nanoflakes. Spin polarization was confirmed by mcAFM and magnetic field-independent magnetic circular dichroism. Because of the magnetic properties of the crystals, the spin selective current results in induced magnetization, so that hysteresis is observed in the current versus voltage curves, similarly to the results obtained with the copper phenylalanine crystals.[56]

III. Discussion

The various materials and systems used for observing the CISS effect differ in size, in composition, and were measured on different substrates, nevertheless similar spin selectivity phenomena were observed. Despite the broad range of chiral materials and the diversity of measurement methods, the experiments reveal a number of shared characteristics that link the material's (or molecule's) chirality and its spin selectivity. We summarize some of these characteristics and discuss a simplified model that may help guide intuition for developing a more precise theory.

Over the past 3 to 4 years, a number of experiments (many of which are discussed above) have shown that the spin filtering in a chiral assembly (or material) is correlated with its chiro-optical response. This body of data reveals that the sense of the spin selectivity (i.e., preference for up spin versus down spin) correlates with the sign of the molecule's (or material's) circular dichroism signal. In fact, the data suggest that this feature is a more robust predictor than are the structural features of the molecules or materials. A number of different studies now exist which show that the magnitude of the spin polarization is proportional to the oscillator strength of the system's lowest energy chiro-optical transition. Optical activity depends on the anisotropic polarizability and a number of experimental studies have now shown the correlation between the spin polarization and the calculated anisotropic polarizability.[76] Whereas recent theoretical work reports enhancement of the spin polarization due to polarons,[15] electron correlation,[13]

and phonons;[77] theoretical efforts have not yet drawn the connection to the circular dichroism response.

The spin polarization arising from CISS manifests whether the electron transport proceeds above the vacuum level (low energy photoemission studies), proceeds through tunneling between bound states, or proceeds through metal-like current flow. While most experimental studies involve electron tunneling steps in the transport, this does not seem to be required. Moreover, various studies show that the spin-polarized transport can proceed over very long range, reaching microns.[19,28,54,55,78] These features suggest that the process need not proceed coherently for the spin filtering to occur and indicates that the spin filtering is not associated only with coherent electron transfer processes. For relatively short distances of up to about 15 nm, the polarization increases about linearly with the length of the system, however beyond this length the spin polarization increases very weakly with the length, if at all. For systems organized in periodic or pseudo-periodic structures, spin selectivity can be maintained for distances exceeding hundreds of nanometers. These observations suggest that two concurrent processes must be operating to generate the observed polarization. The first is the spin from the CISS effect, which keeps filtering the spin all along the conduction path, and the second is spin randomization due to scattering (average spin velocity under electric field). At short distances, the ballistic CISS effect is the dominant process, but the role of scattering increases with the length. A chiral system with long range order can provide a platform for very long-range spin transport, because the chiral potential acts to repetitively repolarize the carriers' spins.

The magnitude of the CISS effect, observed experimentally, cannot be explained by a simple process that assumes conduction of electrons through eigenstates of a chiral system that have spin orbit coupling on the order of few meV, and a need remains to understand the underlying CISS mechanism. One possible approach for a theoretical description was presented recently[2] in which the substrate plays a role. Upon applying an electric field on the chiral system, charge polarization occurs which is accompanied by a small magnitude spin polarization of a few percent. Hence, near the electrode a spin polarization arises. When an additional electron penetrates into the molecule, its spin interacts with the spin distribution near the electrode and the penetration barrier depends on whether the two electrons have opposite or parallel spins, due to the spin exchange

interaction (see Fig. 8). In the first case, the barrier for penetration will be low while for the parallel spins the barrier may be higher by many tens of meV, since the typical exchange interaction is of the order of few eV. This model explains both the correlation of the spin polarization with the anisotropic polarizability of the system as well as the differences in thresholds for injecting opposite spins into the chiral systems (see Fig. 1). By relating the CISS effect to polarization one necessarily includes the electronic component of the polarizability, but other phenomena, e.g. polarons, may play a role.

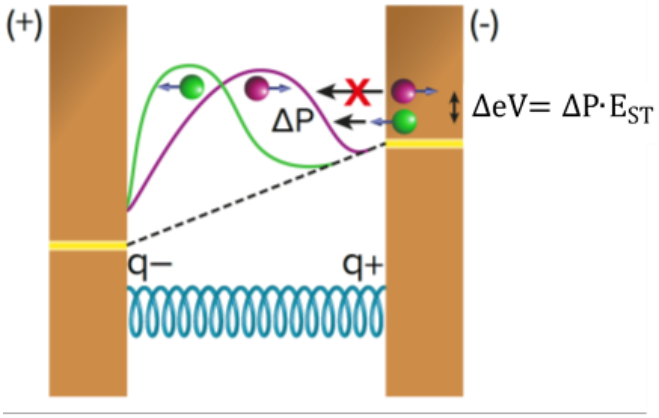

Figure 8: A scheme describing the mechanism of the CISS effect. The effect is presented in terms of a small spin polarization, ΔP, that arises from the spin-orbit coupling. This small spin polarization causes a spin blockade, because of the Pauli principle, which is proportional to the singlet-triplet energy gap, E_{ST}, in the molecule. The purple and green curves represent the charge distribution occurring upon applying the field across the molecule, for electrons with spin aligned parallel (green) or antiparallel (purple) to their velocities. The molecule is presented schematically as a coil. The yellow lines indicate the Fermi energy at each electrode and the dotted line shows the electric field across the molecule, assuming a molecule with a very low dielectric constant. Copied with permission from ref. 2.

Only discovered in 1999, chiral induced spin selectivity refers to the fact that chiral structures (molecules and materials) display a spin dependent interaction with traveling electrons. First observed as a spin-dependent transmission probability for photoelectrons, the phenomenon is now known to manifest in a number of different electron transport processes and for charge displacements, i.e., charge polarization within a chiral molecule generates a spin polarization. CISS appears across a broad spectrum of processes and it has significant implications in biology, chemistry, and materials physics. It is now clear that describing CISS from first principles theory will require a dynamic multielectron

description of spin and charge transport (and displacement). Why was such a fundamental phenomenon overlooked for so long? In part, its observation required the appropriate technological advances to organize and orient chiral molecules (and nanobjects) in ways that their spin-dependent properties could be observed. The advent of nanoscience, and the renaissance it has spawned in materials physics and materials chemistry, has been an important enabler for the discovery of CISS.

Data Available Statement

All the data is either published here or available upon request from the authors.

Acknowledgements

RN and DHW acknowledge the partial support of the US Department of Energy Grant No. ER46430 and the NSF-BSF - 1852588. RN and YP acknowledge the partial support from the Israel Ministry of Science.

III. References

[1] R. Naaman, Y. Paltiel, D. H. Waldeck, "Chiral molecules and the electron spin", *Nature. Rev. Chem.* **3**, 250–260 (2019).

[2] R. Naaman, Y. Paltiel, D. H. Waldeck, "A Perspective on Chiral Molecules and the Spin Selectivity Effect", *J. Phys. Chem. Lett.* **11**, 3660−3666 (2020).

[3] T. S. Metzger, S. Mishra, B. P. Bloom, N. Goren, A. Neubauer G. Shmul, J. Wei, S. Yochelis, F. Tassinari C. Fontanesi D. H. Waldeck, Y. Paltiel, R. Naaman, "The Electron Spin as a Chiral Reagent", *Angewandte Chemie International Edition* **59** 1653 (2020).

[4] K. B. Ghosh, O. Ben Dor, F. Tassinari, E. Capua, S. Yochelis, A. Capua, S.-H. Yang, S. S. P. Parkin, S. Sarkar, L. Kronik, L. T. Baczewski, R. Naaman, and Y. Paltiel, "Enantio-Specific Interaction of Chiral Molecules with Magnetic Substrates", *Science* **360**, 1331–1334 (2018).

[5] S.-H. Yang, "Spintronics on chiral objects", *Appl. Phys. Lett.* **116**, 120502 (2020).

[6] K. Michaeli, N. Kantor-Uriel, R. Naaman, D. H. Waldeck, "The Electron's Spin and Molecular Chirality- How Are They Related and How Do They Affect Life Processes?" *Chem. Soc. Rev.* **45**, 6478 – 6487 (2016).

[7] A. Kumar, E. Capua, M. K. Kesharwani, J. M. L. Martin, E.Sitbon, D. H. Waldeck, R. Naaman, "Chirality-induced Spin Polarization Places Symmetry Constraints on Biomolecular Interactions", *PNAS*, **114**, 2474–2478 (2017).

[8] M. S. Zöllner, S. Varela, E. Medina, V. Mujica, C. Herrmann, "Insight into the Origin of Chiral-Induced Spin Selectivity from a Symmetry Analysis of Electronic Transmission", *J. Chem. Theory Comput*., **16**, 2914–2929 (2020).

[9] Y. Liu, J. Xiao, J. Koo, B. Yan, "Chirality-driven topological electronic structure of DNA-like materials", *Nat. Mat.* (2021). https://doi.org/10.1038/s41563-021-00924-5

[10] A.-M. Guoa, Q.-F. Sun, "Spin-dependent electron transport in protein-like single-helical molecules", *PNAS* **111**, 11658–11662 (2014).

[11] B. P. Bloom, B. M. Graff, S. Ghosh, D. N. Beratan, D. H. Waldeck, "Chirality Control of Electron Transfer in Quantum Dot Assemblies", *J. Am. Chem. Soc.* ***139,*** 9038-9043 (2017).

[12] B. Bloom, R. Liu, P. Zhang, S. Ghosh, R. Naaman, D. Beratan, and D. H. Waldeck "Directing Charge Transfer in Quantum Dot Assemblies" *Accts of Chemical Research* ***51,*** 2565-2573 (2018).

[13] J. Fransson, "Chirality-Induced Spin Selectivity: The Role of Electron Correlations", *J. Phys. Chem. Lett.*, **10**, 7126–7132 (2019).

[14] X. Li, J. Nan, X. Pan, "Chiral Induced Spin Selectivity as a Spontaneous Intertwined Order", *Phys. Rev. Lett*. **125**, 263002 (2020).

[15] L. Zhang, Y. Hao, W. Qin, S. Xie, F. Qu, "Chiral-induced spin selectivity: A polaron transport model", *Phys. Rev. B* **102**, 214303 (2020).

[16] G.-F. Du, H.-H. Fu, R. Wu, "Vibration-enhanced spin-selective transport of electrons in the DNA double helix", *Phys. Rev. B* **102**, 035431 (2020).

[17] V. V. Maslyuk, R.Gutierrez, A. Dianat, V.Mujica, and G. Cuniberti, "Enhanced Magnetoresistance in Chiral Molecular Junctions", *J. Phys. Chem. Lett.* **9**, 5453−5459 (2018).

[18] M. S. Zöllner, A. Saghatchi, V. Mujica, and C. Herrmann, "Influence of Electronic Structure Modeling and Junction Structure on First-Principles Chiral Induced Spin Selectivity", J. Chem. Theory Comput. **16**, 7357−7371 (2020,)

[19] Z. Huang, B. P. Bloom, X. Ni, Z. N. Georgieva, M. Marciesky, E. Vetter, F. Liu, D.H. Waldeck, D. Sun, "Magneto-Optical Detection of Photoinduced Magnetism via Chirality-Induced Spin Selectivity in 2D Chiral Hybrid Organic−Inorganic Perovskites", *ACS Nano*, **14**, 10370−10375 (2020).

[20] C. Fontanesi, E. Capua, Y. Paltiel, D. H. Waldeck and R. Naaman, "Spin-Dependent Processes Measured without a Permanent Magnet" *Adv. Mat*. **30**, 1707390 (2018).

[21] K. Ray, S.P. Ananthavel, D.H. Waldeck, R. Naaman, "Asymmetric Scattering of Polarized Electrons by Organized Organic Films Made of Chiral Molecules", *Science*, **283**, 814-816 (1999).

[22] B. Göhler,V. Hamelbeck, T.Z. Markus, M. Kettner, G.F. Hanne, Z. Vager, R. Naaman, H. Zacharias, "Spin Selectivity in Electron Transmission Through Self-Assembled Monolayers of dsDNA", *Science* **331**, 894-897 (2011).

[23] M. Kettner, B. Göhler, H. Zacharias, D. Mishra, V. Kiran, R. Naaman, C. Fontanesi, D. H. Waldeck, S. Sęk, J. Pawłowski, J. Juhaniewicz, "Spin Filtering in Electron Transport Through Chiral Oligopeptides", *J. Phys. Chem. C*, **119**, 14542−14547 (2015).

[24] M. Kettner, V. V. Maslyuk, D. Nürenberg, J. Seibel, R. Gutierrez, G. Cuniberti, K.-H. Ernst, H. Zacharias, "Chirality-Dependent Electron Spin Filtering by Molecular Monolayers of Helicenes", *J. Phys. Chem. Lett*., **9**, 2025–2030 (2018).

[25] R. A. Rosenberg, J. M. Symonds, V. Kalyanaraman, T. Markus, N. Elyahu, T.M. Orlando, R. Naaman, E. A. Medina, F. A. López, V. Mujica, "Kinetic Energy Dependence of Spin Filtering of Electrons Transmitted Through Organized Layers of DNA", *J. Phys. Chem. C* **117**, 22307−22313 (2013).

[26] D. Nürenberg, H. Zacharias, "Evaluation of spin-flip scattering in chirality-induced spin selectivity using the Riccati equation", *Phys. Chem. Chem. Phys.*, **21**, 3761-3770 (2019).

[27] A. C. Aragonès, E. Medina, M. Ferrer-Huerta, N. Gimeno, M. Teixidó, J. L. Palma, N. Tao, J. M. Ugalde, E. Giralt, I. Díez-Pérez, V. Mujica, "Measuring the Spin-Polarization Power of a Single Chiral Molecule", *Small*, **13**, 1602519 (2017).

[28] U. Huizi-Rayo, J. Gutierrez, J. M. Seco, V. Mujica, I. Diez-Perez, J. M. Ugalde, A. Tercjak, J. Cepeda, E. San Sebastian, "An Ideal Spin Filter: Long-Range, High-Spin Selectivity in Chiral Helicoidal 3-Dimensional Metal Organic Frameworks", *Nano Lett.*, **20**, 8476–8482 (2020).

[29] S. Sanvito, "The Rise of Spinterface Science" *Nature Physics* **6**, 562-564 (2010).

[30] R. Vardimon, M. Klionsky, O. Tal, "Indication of Complete Spin Filtering in Atomic-Scale Nickel Oxide", *Nano Lett.,* **15**, 3894–3898 (2015).

[31] S. Ghosh, S. Mishra, E. Avigad, B. P. Bloom, L. T. Baczewski, S. Yochelis, Y. Paltiel, R. Naaman, D.H. Waldeck, "Effect of Chiral Molecules on the Electron's Spin Wavefunction at Interfaces" *J. Phys. Chem. Letters* **11,** 1550-1557 (2020).

[32] M. Suda, Y. Thathong, V. Promarak, H. Kojima, M. Nakamura, T. Shiraogawa, M. Ehara, H. M. Yamamoto, "Light-driven molecular switch for reconfigurable spin filters", *Nat. Comm*. **10**, 2455 (2019).

[33] S. Mishra, A. K. Mondal, S. Pal, T. K. Das, E. Z. B. Smolinsky, G. Siligardi, R. Naaman, "Length-Dependent Electron Spin Polarization in Oligopeptides and DNA", JPC C 124, 10776-10782 (2020).

[34] X. Yang, C. H. van der Wal, B. J. van Wees, "Spin-dependent electron transmission model for chiral molecules in mesoscopic devices", *Phys. Rev. B* **99**, 024418 (2019).

[35] T. Liu, X. Wang, H. Wang, G. Shi, F. Gao, H. Feng, H. Deng, H. Deng, L. Hu, E. Lochner, P. Schlottmann, S. von Molnár, Y. Li, J. Zhao, P. Xiong, "Linear and Nonlinear Two-Terminal Spin Valve Effect from Chirality-Induced Spin Selectivity", *ACS Nano*, **14**, 15983–15991 (2020).

[36] K. Sarkar, A. Aharony, O. Entin-Wohlman, M. Jonson, R. I. Shekhter, "Effects of magnetic fields on the Datta-Das spin field-effect transistor", *Phys. Rev. B* **102**, 115436 (2020).

[37] O. Entin-Wohlman, A. Aharony, Y. Utsum, Comment on "Spin-orbit interaction and spin selectivity for tunneling electron transfer in DNA", *Phys. Rev. B* **103**, 077401 (2021).

[38] O. Ben Dor, S. Yochelis, S. P. Mathew, R. Naaman, and Y. Paltiel, "A chiral-based magnetic memory device without a permanent magnet", *Nat. Comm*. **4**, 2256 (2013).

[39] S. P. Mathew, P. C. Mondal, H. Moshe, Y. Mastai, R. Naaman, "Non-magnetic Organic/inorganic Spin Injector at Room Temperature", *App. Phys. Lett.* **105**, 242408 (2014).

[40] E. Z. B. Smolinsky, A. Neubauer, A. Kumar, S. Yochelis, E. Capua, R. Carmieli, Y. Paltiel, R. Naaman, K. Michaeli, "Electric field controlled magnetization in GaAs/AlGaAs

heterostructures-chiral organic molecules hybrids", *J. Phys. Chem. Lett*. **10**, 1139–1145 (2019).

[41] I. Meirzada, N. Sukenik, G. Haim, S. Yochelis, L. T. Baczewski, Y. Paltiel, and N. Bar-Gill, "Long-Time-Scale Magnetization Ordering Induced by an Adsorbed Chiral Monolayer on Ferromagnets", *ACS Nano*, **15**, 5574–5579 (2021).

[42] E. Yashima, N. Ousaka, D. Taura, K. Shimomura, T. Ikai, K. Maeda, "Supramolecular Helical Systems: Helical Assemblies of Small Molecules, Foldamers, and Polymers with Chiral Amplification and Their Functions", *Chem. Rev*., **116**, 13752−13990 (2016).

[43] A. R. A. Palmans. E. W. Meijer, "Amplification of Chirality in Dynamic Supramolecular Aggregates", *Angew. Chem. Int. Ed*., **46**, 8948 – 8968 (2007).

[44] P. C. Mondal, C. Fontanesi, D. H. Waldeck, R. Naaman, "Spin-dependent Transport through Chiral Molecules Studied by Spin-dependent Electrochemistry", *Acc. Chem. Res*. **49**, 2560-2568 (2016).

[45] F. Tassinari, D. R. Jayarathna, N. Kantor-Uriel, K. L. Davis, V. Varade, C. Achim, R. Naaman, "Chirality Dependent Charge Transfer Rate in Oligopeptides", *Adv. Mat*. **30**, 1706423 (2018).

[46] L. A. P. Kane-Maguire, G. G. Wallace, "Chiral conducting polymers", *Chem. Soc. Rev*., **39**, 2545–2576 (2010).

[47] E. Yashima, N. Ousaka, D. Taura, K. Shimomura, T. Ikai, K. Maeda, "Supramolecular Helical Systems: Helical Assemblies of Small Molecules, Foldamers, and Polymers with Chiral Amplification and Their Functions", *Chem. Rev*., **116**, 13752−13990 (2016).

[48] P. C. Mondal, N. Kantor-Uriel, S. P. Mathew, F. Tassinari, C. Fontanesi, R. Naaman, "Chiral Conductive Polymers as Spin Filters", *Adv. Mat.* **27**,1924-1927 (2015).

[49] S. Mishra, A. Kumar Mondal, E. Z. B. Smolinsky, R. Naaman, K. Maeda, T. Nishimura, T. Taniguchi, T. Yoshida, K. Takayama, E. Yashima, "Spin Filtering Along Chiral Polymers", *Angew. Chemie* **59**, 2–8 (2020).

[50] D. B. Amabilino, J. Veciana, Supramolecular Chiral Functional Materials, in: Crego-Calama M., Reinhoudt D.N. (eds) Supramolecular Chirality. Topics in Current Chemistry, vol 265 pp 253-302. Springer, Berlin, Heidelberg (2006).

[51] C. Kulkarni, A. K. Mondal, T. K. Das, G. Grinbom, F. Tassinari, M. F. J. Mabesoone, E. W. Meijer, R. Naaman, "Highly efficient and tunable filtering of electrons' spin by supramolecular chirality of nanofiber-based materials", *Adv. Mat*. **32**, 1904965 (2020).

[52] R. Naaman, Y. Paltiel, D.H. Waldeck, "Chiral Induced Spin Selectivity Gives a New Twist on Spin-control in Chemistry", *Acc. Chem. Res*., **53**, 2659−2667 (2020).

[53] B.P. Bloom, Y. Lu, D. H. Waldeck, T. Metzger, S. Yochelis, Y. Paltiel, C. Fontanesi, S. Mishra, F. Tassinari, R. Naaman, "Asymmetric reactions induced by electron spin polarization" *PCCP **22,*** 21570 – 21582 (2020).

[54] H. Lu, J. Wang, C. Xiao, X. Pan, X. Chen, R. Brunecky, J. J. Berry, K. Zhu, M. C. Beard, Z. V. Vardeny, "Spin-dependent charge transport through 2D chiral hybrid lead-iodide perovskites", *Sci. Adv.* **5**, eaay0571 (2019).

[55] H. Lu, C. Xiao, R. Song, T. Li, A. E. Maughan, A. Levin, R. Brunecky, J. J. Berry, D. B. Mitzi, V. Blum, M. C. Beard, "Highly Distorted Chiral Two-Dimensional Tin Iodide Perovskites for Spin Polarized Charge Transport", *J. Am. Chem. Soc.,* **142**, 13030–13040 (2020).

[56] A. K. Mondal, N. Brown, S. Mishra, P. Makam, D. Wing, S. Gilead, Y. Wiesenfeld, G. Leitus, L. J. W. Shimon, R. Carmieli, D. Ehre, G. Kamieniarz, J. Fransson, O. Hod, L. Kronik, E. Gazit, R. Naaman, "Long-Range Spin-Selective Transport in Chiral Metal-Organic Crystals with Temperature-Activated Magnetization", *ACS Nano* **14**, 16624-16633 (2020).

[57] J. Ahn, E. Lee, J. Tan, W. Yang, B. Kim, J. Moon, "A New Class of Chiral Semiconductors: Chiral-Organic-Molecule-Incorporating Organic-Inorganic Hybrid Perovskites". *Mater. Horiz.*, **4**, 851 (2017).

[58] D. Giovanni, H. Ma, J. Chua, M. Grätzel, R. Ramesh, S. Mhaisalkar, N. Mathews, and T. C. Sum "Highly Spin-Polarized Carrier Dynamics and Ultralarge Photoinduced Magnetization in $CH_3NH_3PbI_3$ Perovskite" *Thin Films Nano Lett*., **15**, 1553−1558 (2015).

[59] D. Niesner, M. Wilhelm, I. Levchuk, A. Osvet, S. Shrestha, M. Batentschuk, C. Brabec, and T.Fauster, "Giant Rashba Splitting in $CH_3NH_3PbBr_3$ Organic-Inorganic Perovskite" *Phys. Rev. Lett*., **117**, 126401 (2016**)**.

[60] R. Wang, S. Hu, X. Yang, X. Yan, H. Li and C.X. Sheng. "Circularly polarized photoluminescence and Hanle effect measurements of spin relaxation in organic–inorganic hybrid perovskite films", *J. Mater. Chem. C*, **6**, 2989 (2018).

[61] Y.-H. Kim, Y.Zhai, H. Lu, X. Pan, C. Xiao, E. A.Gaulding, S. P. Harvey, J. J. Berry, Z. V.Vardeny, J. M. Luther, M. C. Beard, "Chiral-induced spin selectivity enables a room-temperature spin light-emitting diode", *Science* **371**, 1129–1133 (2021).

[62] W. Jiang, X. Yia, M. D. McKee, "Chiral biomineralized structures and their biomimetic synthesis", *Mater. Horiz*., **6,** 1974 (2019).

[63] L. Addadi, S. Weiner, "Biomineralization: crystals, asymmetry and life". *Nature* **411**, 753–755 (2001).

[64] H. M. Kothari, E. A. Kulp, S. Boonsalee, M. P. Nikiforov, E. Bohannan, P. Poizot, S. Nakanishi, J. A. Switzer, "Enantiospecific Electrodeposition of Chiral CuO Films from Copper(II) Complexes of Tartaric and Amino Acids on Single-Crystal Au(001)." *Chem. Mater*., **16**, 4232−4244 (2004).

[65] R. Widmer, F.-J. Haug, P. Ruffieux, O. Groening, M. Bielmann, P. Groening, R. Fasel, "Surface Chirality of CuO Thin Films". *J. Am. Chem. Soc*., **128**, 14103−14108 (2006).

[66] L. Xiao, T. An, L. Wang, X. Xu, H. Sun, "Novel Properties and Applications of Chiral Inorganic Nanostructures". *Nano Today*, **30**, 100824 (2019).

[67] A. Visheratina, N. A. Kotov, "Inorganic Nanostructures with Strong Chiroptical Activity", *CCS Chem*., **2**, 583–604 (2020).

[68] J. Kumar, K. G. Thomas, L. M. Liz-Marzán, "Nanoscale chirality in metal and semiconductor nanoparticles", *Chem. Commun.*, **52**, 12555 (2016).

[69] B. P. Bloom, V. Kiran, V. Varade, R. Naaman, D.H. Waldeck "Spin Selective Charge Transport through Cysteine Capped CdSe Quantum Dots", *Nano Lett.* ***16,*** 4583-4589 (2016).

[70] H. Al-Bustami, B. Bloom, A. Ziv, S. Goldring, Sharon; S. Yochelis, R. Naaman, D.H. Waldeck, Y. Paltiel, "Optical Multilevel Spin Bit Device using Chiral Quantum Dots", *Nano Lett.* **20**, 8675–8681 (2020).

[71] A. Inui, R. Aoki, Y. Nishiue, K. Shiota, Y. Kousaka, H. Shishido , D. Hirobe, M. Suda, J. Ohe, J. Kishine, H. M. Yamamoto, and Y.Togawa, "Chirality-Induced Spin-Polarized State of a Chiral Crystal $CrNb_3S_6$", *Phys. Rev. Lett*. **124**, 166602 (2020).

[72] Y. Nabei, D. Hirobe, Y. Shimamoto, K. Shiota, A. Inui, Y. Kousaka,Y. Togawa, H. M. Yamamoto, "Current-induced bulk magnetization of a chiral crystal $CrNb_3S_6$", *Appl. Phys. Lett.* **117**, 052408 (2020).

[73] K. B. Ghosh, W. Zhang, F. Tassinari, Y. Mastai, O. Lidor-Shalev, R. Naaman, P. Möllers, D. Nürenberg, H. Zacharias, J. Wei, E. Wierzbinski, D. H. Waldeck, "Controlling Chemical Selectivity in Electrocatalysis with Chiral CuO Coated Electrodes", *J. Phys. Chem. C*, **123**, 3024-3031 (2019).

[74] S. Ghosh, B. P. Bloom, Y. Lu, D. Lamont, D. H. Waldeck, "Increasing the Efficiency of Water Splitting through Spin Polarization Using Cobalt Oxide Thin Film Catalysts", *J. Phys. Chem. C*, **124**, 22610–22618 (2020).

[75] T. Bai, J. Ai, L. Liao, J. Luo, C. Song, Y. Duan, L. Han, S. Che, "Chiral Mesostructured NiO Films with Spin Polarization", *Angew. Chem.* **60,** (2021). https://doi.org/10.1002/anie.202101069.

[76] H. Su, A.T. Rösch, Q. Zhu, R. Guerrero, R. Naaman, E.W. Meijer, "The dependence of enhanced oxygen evolution on spin polarization and anisotropic polarizability of nitrogen rich compounds", In preparation.

[77] Y. Wu, J. E. Subotnik, "Electronic spin separation induced by nuclear motion near conical intersections", *Nat. Comm.* **12**, 700 (2021).

[78] Md. W. Rahman, K. M. Alam, S. Pramanik, "Long Carbon Nanotubes Functionalized with DNA and Implications for Spintronics", *ACS Omega*, **3**, 17108−17115 (2018).